JOURNAL OF MATERIALS SCIENCE 32 (1997) 2745–2752

Synthesis of a $YBa_2Cu_3O_{7-x}$–Ag composite using a sol–gel method

L. F. ADMAIAI, M. RUWET, P. GRANGE, P. DELMON
Unité de Catalyse et Chimie des Matériaux Divisés, Place Croix du Sud 2/17, 1348 Louvain-la-Neuve, Belgium

M. CASSART, J. P. ISSI
Unité de Physico-Chimie et Physique des Matériaux, Place Croix du Sud 1, 1348 Louvain-la-Neuve, Belgium

The preparation of $YBa_2Cu_3O_{7-x}$–Ag powders by a sol–gel method and the characterization of these powders and also pellets made from these powders is presented. Transmission electron microscopy (TEM) observations show that the silver is highly dispersed in the sample. However, the size of the silver particles in the $YBa_2Cu_3O_{7-x}$ matrix depends largely on the silver concentration in the sample. For low concentrations, the silver particles have sizes of area 10 nm and for higher concentrations the silver particle is larger. The TEM investigations of the powders shows fibre structures for the $YBa_2Cu_3O_{7-x}$–Ag composite. This structure is different from the structures usually observed in the $YBa_2Cu_3O_{7-x}$ system. The microanalysis of these fibres shows that they possess a composition of $YBa_2Cu_3O_{7-x}$. The oxygenation of the samples seems easier in $YBa_2Cu_3O_{7-x}$–Ag composites. The room temperature electrical resistivity of the pellets is decreased by the addition of silver but no enhancement of the superconducting critical temperature is observed.

1. Introduction

Prior to the practical use of polycrystalline bulk $YBa_2Cu_3O_{7-x}$ many problems have to be solved. In particular, high critical current densities (J_c) are necessary for practical applications. The low J_c values currently obtained can be attributed to weak links between grains [1]. Many studies have been performed that have attempted to solve this problem using melt-texturing. This technique tends to reduce the angle between the grains [2–4] thus leading to an increase in J_c values. Other investigated strategies include the introduction of Y_2BaCuO_5 [5–7], silver [8, 9] or SiO_2 [10] as pinning centres for the magnetic flux. The introduction of inclusions is necessary to increase the J_c values even in melt-textured samples in which the grains are aligned. The non superconducting inclusions have to be submicrometer to micrometer in size [11].

In addition to its effect as a pinning centre, silver is also used in $YBa_2Cu_3O_{7-x}$ bulk material for several other reasons. Firstly, it is nearly chemically inert with respect to $YBa_2Cu_3O_{7-x}$ [12]. Secondly, it has been reported that silver enhances the critical current density and reduces the room temperature resistance [13]. In addition to these effects on the electrical properties, silver is also used to improve the mechanical properties of $YBa_2Cu_3O_{7-x}$ because of its ductility and also to increase its thermal conductivity [14]. Silver also has an oxygen diffusion coefficient that is much higher than that for $YBa_2Cu_3O_{7-x}$ in the temperature range where $YBa_2Cu_3O_{7-x}$ has to absorb oxygen in order to become orthorhombic and superconducting [15]. These factors explain why silver has received a considerable amount of attention as a metallic inclusion.

The synthesis of a $YBa_2Cu_3O_{7-x}$–Ag composite by mixing CuO, $BaCO_3$, Y_2O_3 and Ag powders produces silver particles that are too large and inhomogeneously distributed [9, 11]. In order to improve the dispersion of the silver in the $YBa_2Cu_3O_{7-x}$ matrix many alternative synthesis procedures have been proposed for including metallurgical routes such as spray drying [10] and the sol–gel method [16]. However, to the best of our knowledge, a higher dispersion level of the silver has not been obtained and the study of microstructures of $YBa_2Cu_3O_{7-x}$–Ag powders prepared by methods other than metallurgical routes have yet to be reported.

In this work we propose a preparation procedure for a $YBa_2Cu_3O_{7-x}$–Ag composite and the characterization of the powders and pellets. The powders are characterized by X-ray diffraction (XRD) and transmission electron microscopy (TEM). The pellets are characterised by X-ray diffraction, scanning electron microscopy (SEM) and electrical measurements. The results of the microstructural investigations show a particular shape of the particle and a high level of silver dispersion. At low silver concentrations, the silver particle sizes are of the order of a nanometer. At higher silver concentrations, agglomerated silver

0022–2461

particles are formed. The influence of silver on the electrical properties is also demonstrated.

2. Experimental procedure

2.1. Synthesis procedure

The yttrium, barium and copper acetates and the silver nitrate were supplied by Aldrich (99.99%). A 200 mg^{-1} solution of the Y, Ba and Cu elements (Y:Ba:Cu = 1:2:3) in acetic acid:water, 2.5:1, was prepared with stirring at 80 °C. One preparation was performed without the addition of any silver whilst three solutions were prepared with different amounts of silver, in order to obtain 1.6, 3.3 and 6.5 wt % of silver in the final product. Ammonia was used to adjust the pH to 4.4 and the solutions were heated at 80 °C for 16–24 h until a viscous liquid was obtained following the slow water evaporation.

The prepared gels were dried in a vacuum oven at 50, 100 and 150 °C successively. The total drying time was 36 h and the resulting green solids were calcined at 300 °C for 4 hs. The resulting black powders were subsequently calcined for 6 h either at 920 °C if they contained silver or 870 °C if they contained no added silver in a tube furnace under an oxygen flow of 60 ml min^{-1}.

The calcined powders, were formed into pellets by pressing at 7.8 10^8 Pa for 3 min and these pellets were then calcined at 940 °C for 6 h and annealed at 475 °C in a flowing oxygen atmosphere (60 ml min^{-1}) for 16 h for the sample prepared without silver and 12 h for the samples prepared with silver.

2.2. Characterization techniques

The different powders were characterized by XRD (Siemens D-5000 diffractometer using CuK_α radiation and a scan rate of 1° 2θ min^{-1} and TEM (Jeol 100CX Temscan). For elemental analysis an Energy dispersive X-ray spectrometer (EDX) was used. The pellets were characterized by SEM (Lieca stereo scan 260), XRD and by electrical resistivity measurements.

3. Results

3.1. XRD of the powders

Fig 1a shows the spectra of the $YBa_2Cu_3O_{7-x}$ composites with 0, 1.6, 3.3 and 6.5 wt % of silver calcined at 920 °C for 6 h. We note that in this figure all the $YBa_2Cu_3O_{7-x}$ samples have an orthorhombic structure.

The diffraction peaks for silver are located at 38, 44 and 64°. The intensities of these peaks are almost the same for the different samples whatever the silver concentration. This result suggests a high level of dispersion of the silver in the samples. The width of the peaks is greater for the sample prepared without silver compared to the sample prepared with silver. This means that the $YBa_2Cu_3O_{7-x}$ crystallites are smaller when silver is present in the powder. Thus the dispersed silver inhibits the growth of $YBa_2Cu_3O_{7-x}$ grains.

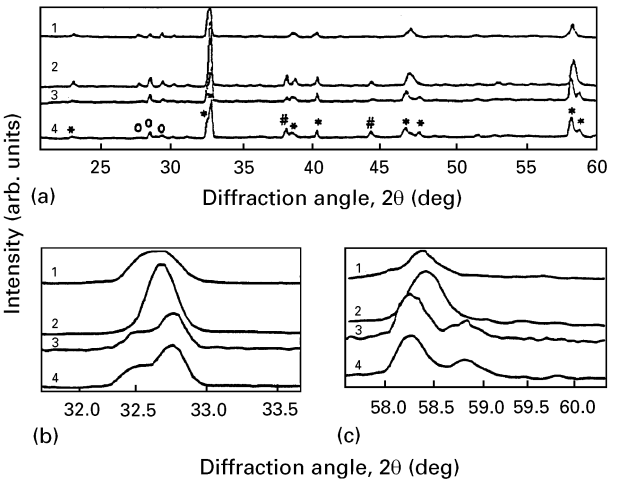

Figure 1 (a) XRD spectra of powders prepared with (1), 0 (2) 1.6, (3) 3.3 and (4) 6.5 wt % of silver and calcined at 920 °C for 6 h. (∗) $YBa_2Cu_3O_{7-x}$, (#) silver and (○) unidentified phase, (b) and (c) are expanded sections of (a).

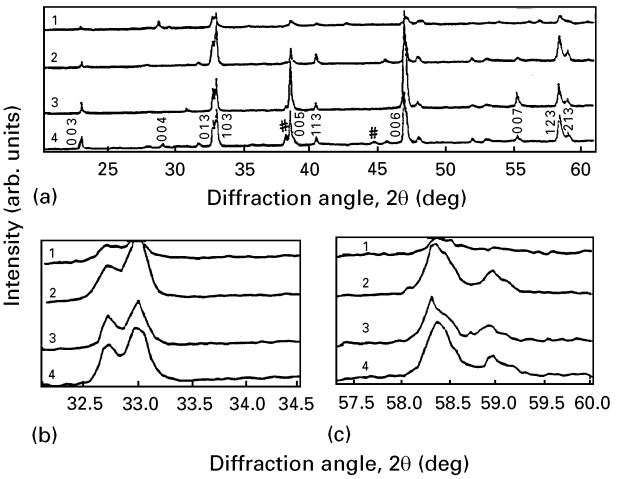

Figure 2 (a) XRD spectra of pellets containing (1) 0, (2) 1.6, (3) 3.3 and (4) 6.5 wt % of silver. (#) silver indexed peaks belong to $YBa_2Cu_3O_{7-x}$, (b) and (c) are expanded sections of (a).

$YBa_2Cu_3O_{7-x}$ samples with 3.3 and 6.5 wt % silver exhibit a high level of orthorhombic splitting of the peaks. By expanding the range between (32–35°) Fig. 1b and (57–60°) Fig. 1c we could easily identify the (013) and (103) peaks located at 32.5 and 32.8° respectively. One should bear in mind that these samples have not been annealed in an oxygen atmosphere. This result confirms that the silver promotes oxygenation of $YBa_2Cu_3O_{7-x}$ crystallites in agreement with what has been previously reported in the literature [12]. In addition to the diffraction peaks of orthorhombic $YBa_2Cu_3O_{7-x}$ and silver peaks there is a small amount of an unidentified phase. By comparing with ASTM standards, this phase could not be attributed to any other cuprate such as $BaCuO_2$ and Y_2BaCuO_5.

3.2. XRD of the pellets

Fig. 2(a–c) presents the spectra of $YBa_2Cu_3O_{7-x}$–Ag composite pellets calcined at 920 °C for 6 h and

annealed at 475 °C for 12 h. For comparison the sample prepared without silver and annealed at 475 °C for 16 h is also displayed.

The orthorhombic splitting of the peaks is more pronounced in these spectra than in the spectra of the powder samples, especially for the pellet prepared with the $YBa_2Cu_3O_{7-x}$ composite. In addition the degree of splitting is greater in the spectrum of the sample containing the highest Ag content. The splitting is also present in the spectrum of the pellet prepared without any added silver however this pellet needed a longer annealing time to attain a high level of oxygenation.

The spectra shown in Fig. 2a principally display diffraction peaks that can be assigned to silver and orthorhombic structured $YBa_2Cu_3O_{7-x}$. Fig. 2(b and c) are obtained by expanding the range between 32–34° and 57–60° respectively, the intensities of the (0 0 1) peaks are higher compared to those in the spectra of the powder. This means that the grains grow anisotropically as plate like entities and are partially oriented in the pellet. However there is no correlation between the intensity of the (0 0 1) peaks and the amount of silver in the samples. The XRD result should however be confirmed by scanning electron microscopy.

3.3. Microstructural analysis

3.3.1. Scanning electron microscopy

Fig. 3(a–d) shows scanning electron micrographs of cross-sections of the pellets. In these pictures we observe different sized plate-like grains that are connected together and clean grain boundaries. Apparently, there is no difference between the samples prepared with or without silver in that all the pellets have plate-like structures. EDX analysis of different pellets, Fig. 3(e–g), showed that the silver peak is always associated with the Y, Ba and Cu peaks. There is no evidence of segregated silver particles. This is true even for the pellets containing high concentration of silver. The analysis was performed in the centre of the particles and at the interfaces between them. The silver is highly dispersed in the sample and strongly associated with the $YBa_2Cu_3O_{7-x}$ matrix. Consequently, it was not possible to detect isolated silver particles in the samples by scanning electron microscopy.

3.3.2. Transmission electron microscopy

In order to determine the silver dispersion and to study the microstructure of the samples, transmission electron microscopy was performed on the powder samples. The result of this analysis is shown in Fig. 4(a–f) for the samples calcined at 920 °C for 6 h. It proved possible to identify four different structures in all the investigated samples. Fig. 4a displays the micrograph of the sample prepared with 1.6 wt % silver. This micrograph shows that the size of the silver particle is 10 mm (dark point) and that the $YBa_2Cu_3O_{7-x}$ grain size is 600 nm. The silver particle has a different aspect compared to the $YBa_2Cu_3O_{7-x}$ grain and is localized on the $YBa_2Cu_3O_{7-x}$ matrix. The silver particles are highly associated to the $YBa_2Cu_3O_{7-x}$ matrix.

Fig. 4b shows the micrograph of the sample prepared with 3.3 wt % silver. In this picture, two different kinds of solid particles can be observed namely spherical and agglomerated particles. The microanalysis shows that the first particle is silver and the second one is $YBa_2Cu_3O_{7-x}$. In this sample the silver particle size is 70 nm and the $YBa_2Cu_3O_{7-x}$ particle size is 740 nm. The silver particle size is 7 times larger than that of the previous sample. Comparing the sample prepared with a low silver concentration to the sample with a higher concentration it can be noted that the silver particle size increases with increasing silver concentration. The $YBa_2Cu_3O_{7-x}$ particles consist of small agglomerated particles. In this micrograph we did not observe any other particle structures.

Fig. 4(c–e) show the $YBa_2Cu_3O_{7-x}$–Ag composites prepared with 1.6, 3.3 and 6.5 wt % of silver respectively. These micrographs show particles with a tubular structure, particularly in the case of the samples prepared with 3.3 and 6.5 wt % silver. This structure is similar to the twin structure previously reported in the literature. The twins are generally observed by transmission electron microscopy and consist of sharp streaks of diffuse scattering along the (0 0 1) directions at Bragg peaks. These should not be confused with the tweed structure which is observed in oxygen deficient samples. Since the twins in the (0 0 1) direction are created by overlapping lentacular domains along the (1 1 0) directions [17].

It is worth reiterating that all the samples have not been annealed in an oxygen atmosphere. However, Fig. 4d corresponding to $YBa_2Cu_3O_{7-x}$–Ag containing 3.3 wt % silver shows two different particles namely $YBa_2Cu_3O_{7-x}$ particles (clear part) composed of a cross fibre structure and silver particles (dark part) and on the surface around this particle there are isolated needle shaped $YBa_2Cu_3O_{7-x}$. Fig. 4(e and f) show micrographs of the $YBa_2Cu_3O_{7-x}$–Ag composite containing 6.5 wt % silver. This particle has a fibre-like structure. In the case of Fig. 4f the fibres in this particle consist of boxed structures. We also note the dispersed silver particles attached to the fibre. The size of the fibre around this particle can reach 2.5 μm in length and 0.1 μm in width. The silver particle size is 70 nm.

Fig. 5 consists of a micrograph of a $YBa_2Cu_3O_{7-x}$ composite containing 3.3 wt % silver calcined at 870 °C. In the edge of this particle we note the needle radiating out from the particle. The length of this needle is 2.5 μm with a width of 30 nm.

Fig. 6(a and b) are micrographs of a $YBa_2Cu_3O_{7-x}$ sample prepared without silver and calcined at 870 °C. The grains consist of disordered needle shaped particles mixed together. The EDX analysis of this particle at different positions shows a homogeneous $YBa_2Cu_3O_{7-x}$ composition. The particle size of the grain in Fig. 6a is approximately 2 μm. Around this particle a needle structure is easily observed and the length of these needles can reach 420 nm with a width of 27 nm. The needle structures are also observed inside the grain. This observation suggests that this

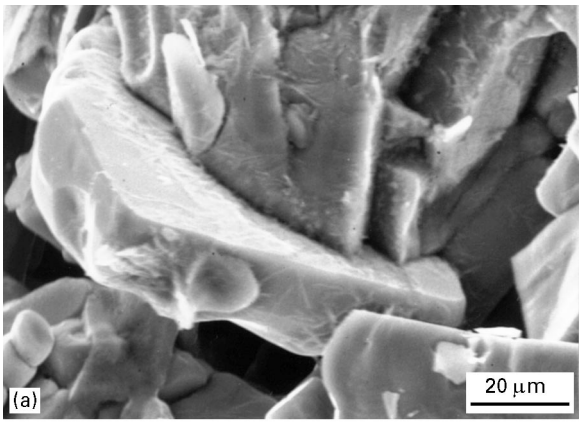

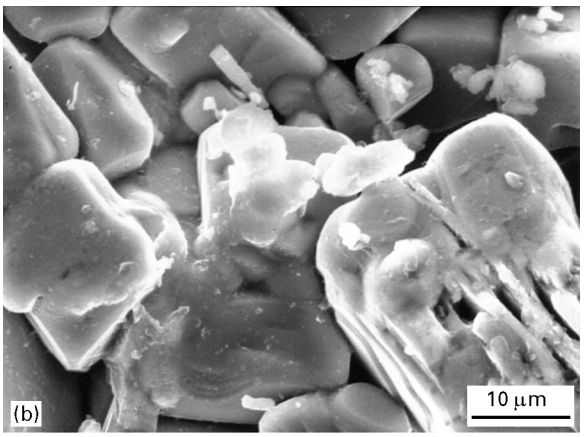

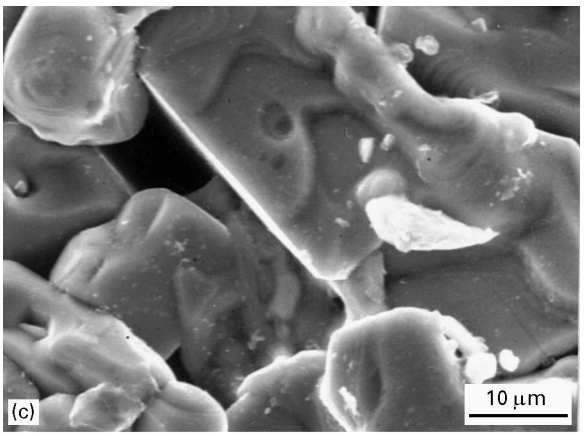

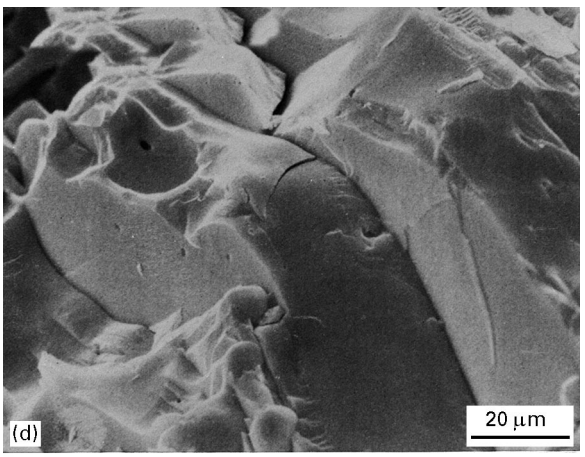

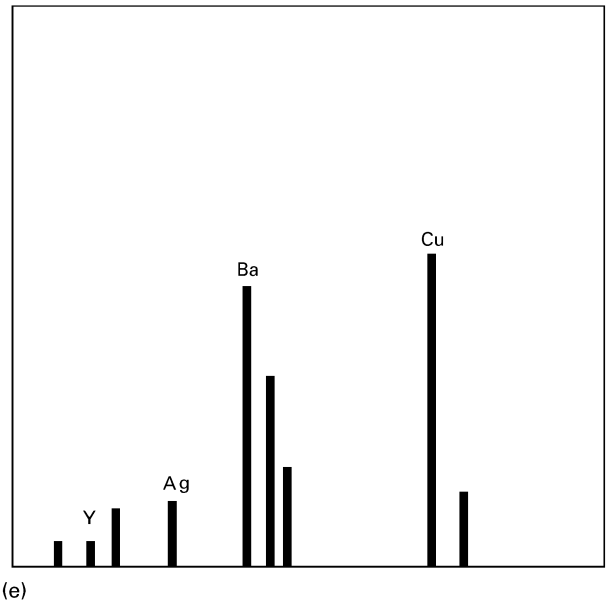

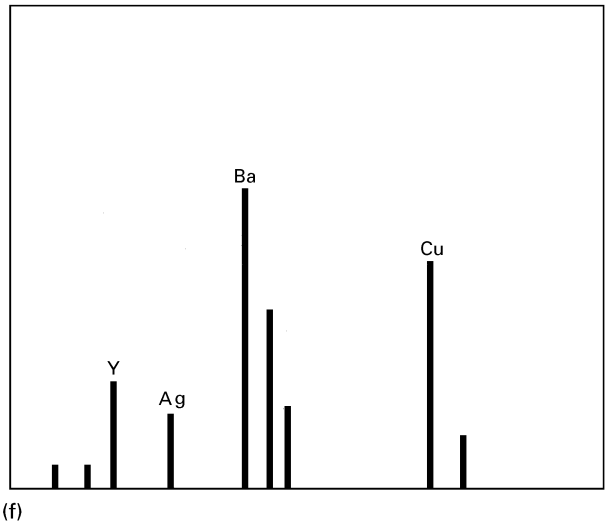

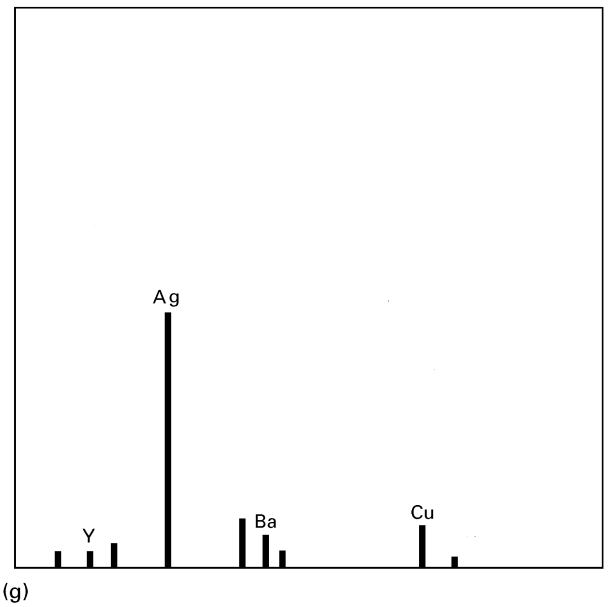

Figure 3 SEM micrographs of the pellets prepared with (a) 1.6, (b) 3.3, and (c) 6.5 wt % silver calcined at 940 °C and annealed at 475 °C for 16 h. (d) is a $YBa_2Cu_3O_{7-x}$ pellet prepared without silver. (e, f, g) are the corresponding EDX spectra.

grain consists of the association of needle-shaped structures. Fig. 6b provides evidence that the grain is composed of small crystallites. The size of these crystallites is around 210 nm in length and 70 nm in

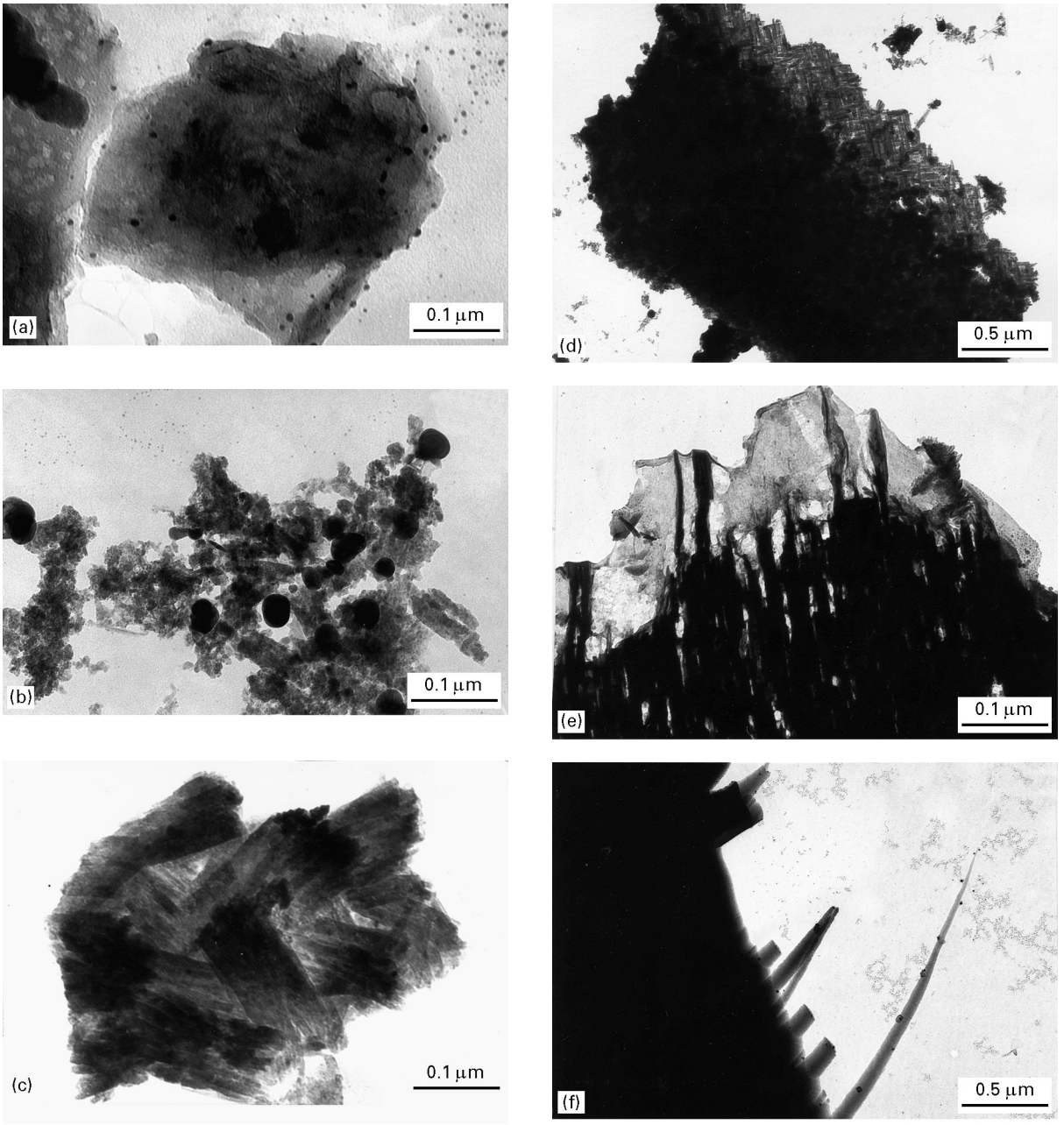

Figure 4 TEM micrographs of powders prepared with (a) 1.6, (b) 3.3 wt % silver and (c) 1.6, 3.3 (d) and (e, f) 6.5 wt % silver calcined at 920 °C for 6 h.

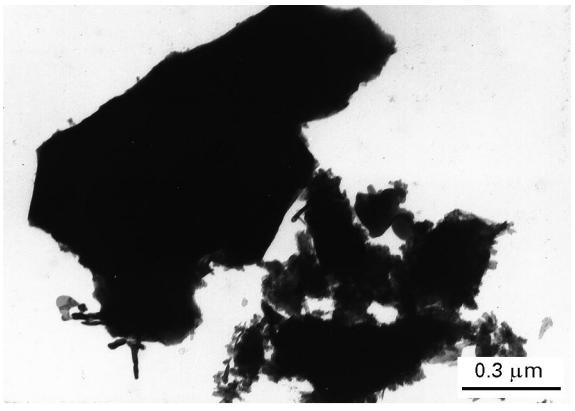

Figure 5 TEM micrograph of powder prepared with 3.3 wt % silver and calcined at 870 °C.

width. Fig. 6(c and d) are micrographs of a $YBa_2Cu_3O_{7-x}$ sample prepared without silver and calcined at 920 °C. On these micrographs we note that this particle consists of a needle shaped structure which is quite similar to the sample calcined at 870 °C. However, the size of these needles is higher than those observed in Fig. 6(a and b). A microanalysis performed at various points in these samples shows a composition of $YBa_2Cu_3O_{7-x}$. It should be noted that the samples were sensitive to the electron beam during the measurements.

3.4. Electrical resistivity measurements

Fig. 7(a and b) show the results of electrical resistivity measurement on the $YBa_2Cu_3O_{7-x}$ samples containing 0, 1.6, 3.3 and 6.5 wt % silver. We note in this figure that the room temperature resistivity drastically decreases with increasing silver concentrations.

At room temperature the resistivity of the pellets are around 10^{-3}, 10^{-7} and $10^{-8}\,\Omega\,m$ for samples containing 1.6, 3.3 and 6.5 wt % silver respectively. The resistivity of the sample prepared without silver is

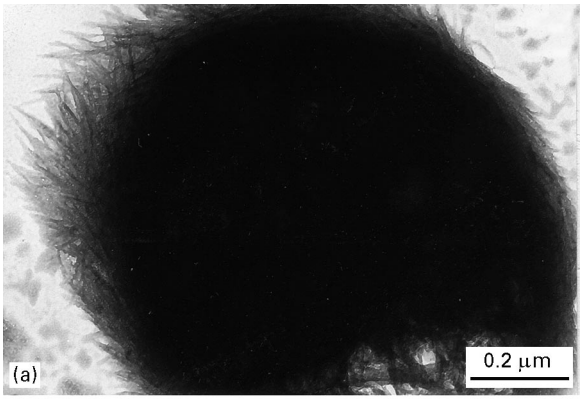

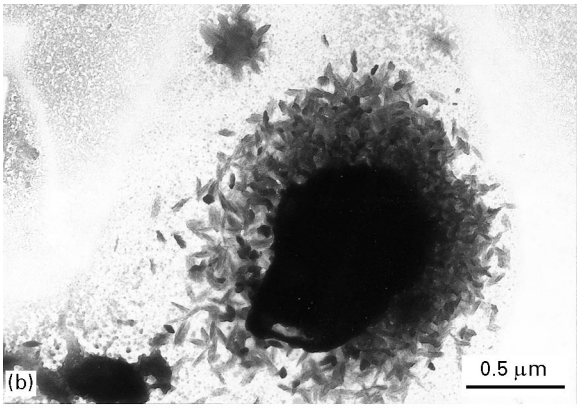

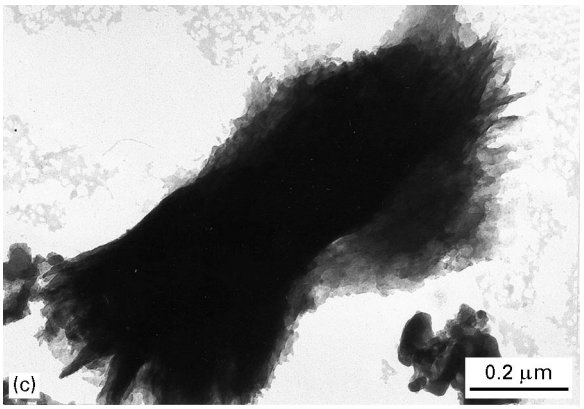

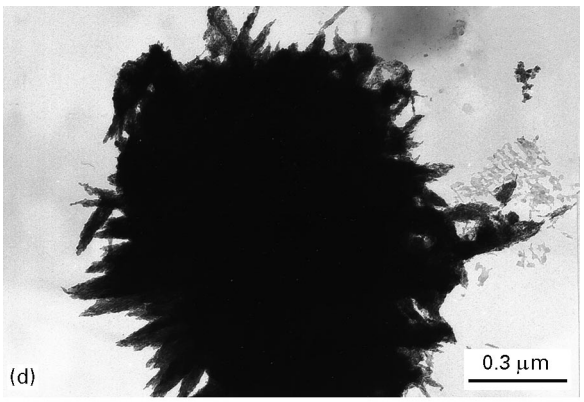

Figure 6 TEM micrographs of powders without silver and calcined at 870 °C (a and b) or at 920 °C (c and d).

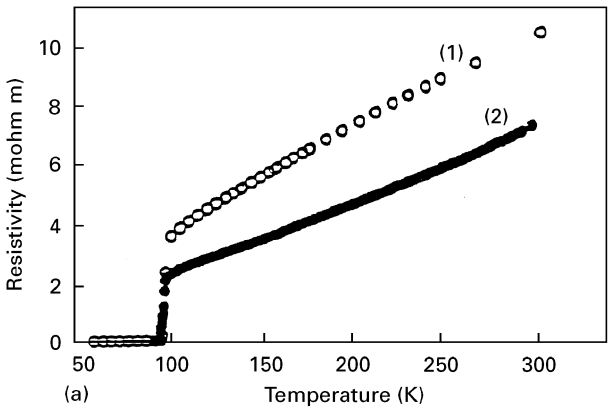

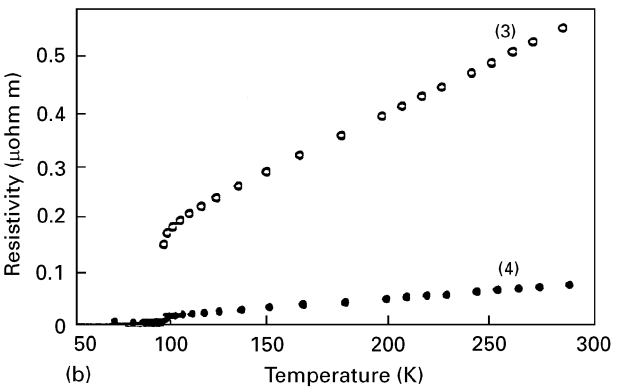

Figure 7 Electrical measurement of pellets containing (1) 0, (2) 1.6, (3) 3.3 and (4) 6.5 wt % of silver.

$10^{-2}\,\Omega\,m$ and thus obviously the silver has a beneficial effect on the room temperature resistivity.

Decreasing the measuring temperature induces a linear decrease in the resistivity until at 92 K the sample becomes superconducting. The critical temperature T_c was 92 K for all the samples and did not change with the Ag content which is contrast to a report of an enhancement in the critical temperature with silver content [18].

4. Discussion

The microstructural characterization of $YBa_2Cu_3O_{7-x}$, especially the identification of defects, is very important if an understanding of their behaviour is to be attained. The defects particularly affect the tetragonal–orthorhombic phase transformation and also the nature and concentration of defects determines some of the electrical properties such as the critical current density. The electron microscopy study of the powder obtained by the sol–gel method shows large differences in the morphology for the different preparations. In the following sections we will discuss the results and compare them with those reported in the literature. This comparison is difficult since in the literature the microstructural characterizations are generally performed on thin pellets. We shall initially discuss the effect of the silver on the oxygenation of $YBa_2Cu_3O_{7-x}$, the dispersion of silver and the effect of silver on the particle growth and its role on the microstructure.

4.1. The effects of silver on the oxygenation of $YBa_2Cu_3O_{7-x}$

XRD spectra of both powders and pellets confirm that the orthorhombic splitting of the peaks is more pronounced in the silver containing samples.

We now discuss the crystallographic structure of $YBa_2Cu_3O_{7-x}$ and the effect of silver on it.

During the synthesis, $YBa_2Cu_3O_{7-x}$ crystallizes at high temperature as a tetragonal structure. During slow cooling or annealing in an oxygen atmosphere the level of oxygen in the sample increases and the structure changes to orthorhombic symmetry. This oxygen fixation is slow because of the low diffusion coefficient of oxygen in $YBa_2Cu_3O_{7-x}$. The solubility of oxygen is higher in the presence of silver leading to an improvement of $YBa_2Cu_3O_{7-x}$ oxygenation [15].

Actually, $YBa_2Cu_3O_{7-x}$ can be considered to be an oxygen deficient perovskite structure since $YBa_2Cu_3O_7$ requires 2 oxygen atoms to reach the stoichiometric $3ABO_3$ perovskite structure [19]. The oxygen level in $YBa_2Cu_3O_{7-x}$ can change from 6 to 9. In the range of 6 to 6.4 $YBa_2Cu_3O_{7-x}$ is tetragonal with semiconducting electrical behaviour. From 6.5 to 6.8 $YBa_2Cu_3O_{7-x}$ is orthorhombic with a T_c of 60 K. From 6.8 to 7 the $YBa_2Cu_3O_{7-x}$ is orthorhombic and T_c is 92 K. When the level of oxygen is higher than 7, the material is tetragonal with a semiconducting behaviour [20].

4.2. The dispersion of the silver in the sample

For low silver concentrations, the very small particles are homogeneously distributed and highly dispersed in the $YBa_2Cu_3O_{7-x}$ matrix. During the melt texturing of $YBa_2Cu_3O_{7-x}$–Ag composite pellets the silver plays the role of a pinning centre. This happens when the particle size is less than 1 μm. These particle sizes are much smaller than those obtained when the solids are prepared by conventional solid state reaction. In these conditions the silver particle size is much higher than 1 μm and the silver particles have a tendency to agglomerate into clusters separated from the $YBa_2Cu_3O_{7-x}$ composite. Thus, in that case, the silver could not act as a pinning centre and thus J_c did not increase [11].

By using the sol–gel method it is possible to get highly dispersed silver when the concentration of silver is low (1.6 wt % silver). This high level of dispersion could originate from Ag–Cu interactions and the formation of Ag–Cu mixed compounds during the calcination process [10]. Furthermore, silver can be accomodated in the $YBa_2Cu_3O_{7-x}$ structure by the substitution of Ag for Cu but the amount of substitution is low [21].

When the amount of silver is higher, the silver particles agglomerate. The agglomeration of silver particles enhances the mechanical properties such as ductility.

For our samples it was experimentally confirmed that fine silver particles of 10 nm in size were dispersed into the $YBa_2Cu_3O_{7-x}$ matrix. This is especially true when the concentration of silver is low. Thus this sample could be used as a precursor for a melt-textured pellet. In the sample with a higher silver content both dispersed silver particles and agglomerates are observed.

4.3. Effect of silver on the $YBa_2Cu_3O_{7-x}$ grain growth

The XRD spectra in Fig. 2(a–c) exhibits high intensities of the (0 0 1) peaks. In the literature, the XRD of pellets are generally the same as that of powders and scanning electron micrographs do not show plate-like grains [22, 23]. Our results confirm that using the sol–gel method the grains quickly grow in the (*ab*) plane and the grains adopt a brick-like shape. This is true for all the pellets prepared using the sol–gel method. Apparently, the addition of silver does not affect the grain growth.

4.4. Shape and microstructure of the grains prepared without silver

In the sample of $YBa_2Cu_3O_{7-x}$ prepared without silver we only identified twin free needle-shaped particles that have also been observed by other workers [24]. Fagan *et al.* identified a needle shaped structure, similar to that observed in our case, in particles prepared by the sol–gel method and coated by titanium oxide [25]. They attempted to explain the formation of this structure in terms of the presence of the titania. However, in their case the SEM and TEM observations did not provide any evidence of the presence of titanium in the needle-shaped grains even in the sample prepared with the highest concentration of titanium oxide. Furthermore, the needle shaped structure in their case was also present at low concentrations of the titanium oxide.

In our case the powder prepared without silver and calcined at 920 °C presents the same aspect as that observed by Fagan *et al.* and our preparation did not contain any titania. Furthermore, the microanalysis of the sample reveals a composition of $YBa_2Cu_3O_{7-x}$ without any contamination. Thus, the formation of the needle-shaped structure is independent of any titania present in the sample.

The micrograph of the $YBa_2Cu_3O_{7-x}$ sample prepared without silver and calcined at 870 °C demonstrates that the $YBa_2Cu_3O_{7-x}$ also crystallizes in a needle-shaped structure. The difference between the samples calcined at 870 and 920 °C is that the extent of sintering is smaller at lower temperature. Thus, the needles observed in the sample calcined at 870 °C are thinner. This observation leads us to think that the thin needle-shape is created during the first step of the formation of $YBa_2Cu_3O_{7-x}$ and that during the heat treatment the needle shape size increase until the solid particle, as shown in the SEM micrographs, is formed.

In the case of $YBa_2Cu_3O_{7-x}$ samples obtained by mixing CuO, $BaCO_3$ and Y_2O_3 powders and repeated heating and grinding, information about the initial stages of formation of the particle shape is lost. By comparison with the method used in this work the yttrium, barium and copper are highly mixed and there is no repeated heating and grinding. Thus, the initial structure of the $YBa_2Cu_3O_{7-x}$ particle is preserved. This could be the reason for this particular structure.

4.5. Shape and microstructure of the samples prepared with silver

The samples prepared with silver, show a needle structure similar to a twin but these needles are not structured. The twin structure appears in the sample because of the tetragonal–orthorhombic crystallographic transition. In fact $YBa_2Cu_3O_{7-x}$ crystallizes at high temperature (900 °C) in a tetragonal structure but during the cooling and annealing in an oxygen atmosphere in the 400–500 °C range the tetragonal structure changes to an orthorhombic structure. In the tetragonal structure the unit cell has $a = b \neq c$ but in the orthorhombic structure $a \neq b \neq c$. The strain that accompanies this structural modification leads to the formation of the twinned structure [26, 27]. The twins, generally observed by TEM, are the sharp streaks of diffuse scattering along the (1 1 0) directions at Bragg peaks [24]. This is different to the tweed structure that is observed in oxygen deficient samples.

However, the structure observed in our samples could not be either twin or tweed structures because, during the TEM analysis, the samples are tilted at different angles and we did not observe any changes in the structure. We observe the morphology of the sample and the structure of the fibres consists of both straight and curved shapes that are sensitive to the electron beam.

4.6. Effect of silver on the $YBa_2Cu_3O_{7-x}$ microstructure

If we compare the micrographs of the sample prepared without silver and calcined at 870 °C and the sample prepared with silver and calcined at 920 °C we note that both structures are quite similar. The needle shapes are present in both samples. This observation leads us to conclude that, in the sample containing the silver, the thickness of the needle shape is small even if the sintering temperature is high. The needle shapes in the sample prepared with silver are more structured. We are unable to explain this behaviour.

5. Conclusions

The present study allows to conclude that:

(1) The XRD measurements show a high level of oxygenation for the samples prepared with silver.

(2) The microstructural analysis of different samples show that the silver is highly dispersed in the $YBa_2Cu_3O_{7-x}$ matrix. The particle size of the silver depends on its concentration even though the sol–gel method produces a high homogeneity. At low silver concentrations, the silver particle size has an area of 10 nm. Thus in order to use the silver as a pinning centre in $YBa_2Cu_3O_{7-x}$ it is necessary to work with a very low silver concentration.

(3) The samples prepared with and without silver contain a needle shaped structure. The microanalysis of several of these needle shapes shows that they possess a composition of $YBa_2Cu_3O_{7-x}$.

(4) The presence of silver decreases the room temperature electrical resistivity. No enhancement of the critical temperature with an increasing silver content was observed.

Acknowledgements

The financial support of the "Service de la programmation de la Politique Scientifique" Belgium is gratefully acknowledged.

References

1. S. KUHARUANGRONG and J. TAYLOR, *J. Amer. Ceram. Soc.* **74** (1991) 1964.
2. M. R. LEES, P. de RANGO, D. BOURGAULT, J. M. BARBUT, D. BRAITHWITE, P. LEJAY, A. SULPICE and R. TOURNIER, *Supercond. Sci. Technol.* **5** (1992) 362.
3. S. JIN, G. W. KAMMLOTT, T. H. TIEFEL and S. K. CHEN, *Physica C* **198** (1992) 33.
4. M. A. RODRIGUEZ, B. J. CHEN and R. L. SNYDER, *ibid.* **195** (1992) 185.
5. A. GOYAL, W. C. OLIVER, P. D. FUNKENBUSCH, D. M. KROEGER and S. G. BURNS, *ibid.* **183** (1991) 221.
6. T. IZUMI, Y. NAKAMURA, T. H. SUNG and Y. SHIOHARA, *J. Mater. Res.* **7** (1992) 801.
7. D. BOURGAULT, P. de RANGO, J. M. BARBUT, D. BRAITHWITE, M. R. LEES, P. LEJAY, A. SULPICE and R. TOURNIER, *Physica C* **194** (1992) 171.
8. J. J. CALABRESE, M. A. DUBSON and J. C. GARLAND, *J. Appl. Phys.* **72** (1992) 2958.
9. D. LEE, X. CHAUD and K. SALAMA, *Jpn. J. Appl. Phys.* **31** (1992) 2411.
10. Y. TAKAO, M. AWANO and H. TAKAGI, *J. Mater. Res.* **7** (1992) 2942.
11. M. MIRONOVA, D. F. LEE and K. SALAMA, *Physica C* **211** (1993) 188.
12. M. MURAKAMI, *Supercond. Sci. Technol.* **5** (1992) 185.
13. M. ITOH, H. ISHIGAKI, T. OHYAMA, T. MINRMOTO, H. NOJIRI and M. MOTOKAWA, *J. Mater. Res.* **6** (1993) 2272.
14. L. RYLANDT, M. CASSART, A. VANDENBOSH, F. DELANNAY and J. P. ISSI, *Mater. Res. Soc. Symp. Proc.* **169** (1990) 1243.
15. B. C. HENDRIX, T. ABE, J. C. BOROFKA, P. C. WANG and J.K. TIEN, *J. Amer. Ceram. Soc.* **76** (1993) 1008.
16. M. K. AGARWALA, D. L. BOURELL and C. PERSAD, *ibid.* **75** (1992) 1975.
17. Y. ZHU, J. TAFTO and M. SUENAGA, *MRS Bull.* **16** (1991) 54.
18. M. AWANO, K. KANI, Y. TAKAO, Y. KUWAHARA and H. TAKAGI, *J. Mater. Res.* **7** (1992) 3185.
19. A. R. WEST, in "Basic solid state chemistry" (J. Wiley and Sons, Chichester, 1988) p. 290.
20. D. J. ROTH, M. R. DEGUIRE and L. E. DOLHERT, *J. Amer. Ceram. Soc.* **75** (1992) 1182.
21. J. JOO, J. P. SINGH, R. B. POEPPEL, A. K. GANGOPADHYAY and T. O. MASON, *J. Appl. Phys.* **71** (1992) 2351.
22. N. L. WU and E. RUCKENSTEIN, *Mater. Lett.* **5** (1987) 432.
23. M. AWANO, K. KANI, Y. TAKAO and H. TAKAGI, *Jpn. J. Appl. Phys.* **30** (1991) L802.
24. L. F. ADMAIAI, L. DAZA, P. GRANGE and B. DELMON, *J. Mater. Sci. Lett.* **13** (1994) 668.
25. J. G. FAGAN and V. R. W. AMARAKOON, *J. Mater. Res.* **8** (1993) 1501.
26. M. SARIKAYA, I. A. AKSAY and R. KIKUCHI, *Mat. Res. Soc. Symp. Proc.* **169** (1990) 805.
27. O. R. MONTEIRO, *J. Amer. Ceram. Soc.* **73** (1990) 1159.

Received 17 March 1995
and accepted 21 October 1996